JOURNAL OF MATERIALS SCIENCE 33 (1998) 1325–1332

High-temperature slow crack growth of silicon carbide determined by constant-stress-rate and constant-stress testing

SUNG R. CHOI*
Cleveland State University, Cleveland, OH 44115, USA
E-mail: sung.r.choi@lerc.nasa.gor

J. A. SALEM, N. N. NEMETH
Lewis Research Center, National Aeronautics and Space Administration, Cleveland, OH 44135, USA

High-temperature slow-crack-growth behaviour of hot-pressed silicon carbide was determined using both constant-stress-rate (''dynamic fatigue'') and constant-stress (''static fatigue'') testing in flexure at 1300 °C in air. Slow crack growth was found to be a governing mechanism associated with failure of the material. Four estimation methods such as the individual data, the Weibull median, the arithmetic mean and the median deviation methods were used to determine the slow crack growth parameters. The four estimation methods were in good agreement for the constant-stress-rate testing with a small variation in the slow-crack-growth parameter, n, ranging from 28 to 36. By contrast, the variation in n between the four estimation methods was significant in the constant-stress testing with a somewhat wide range of $n = 16$ to 32. © *1998 Chapman & Hall*

1. Introduction

Advanced ceramics are candidate materials for high-temperature structural applications in heat engines and heat recovery system. One of the major limitations of these materials in high-temperature applications is delayed failure, where slow crack growth of inherent flaws can occur until a critical size for catastrophic failure is attained. Therefore, it is important to evaluate accurately slow-crack-growth behaviour with a specified loading condition so that reasonable lifetime prediction of ceramic components is ensured.

There are several ways of determining the slow crack growth of a ceramic material. Typically the slow crack growth of ceramics is determined by applying a constant stress-rate ("dynamic fatigue"), a constant stress ("static fatigue" or "stress rupture") or cyclic loading ("cyclic fatigue") to smooth specimens or to pre-cracked fracture mechanics specimens in which the crack velocity measurements are made. A considerable amount of research has been carried out to characterize the slow-crack-growth behaviour of ceramic materials using the testing methods mentioned above [1–8]. Although the reported results generally agree, there remain uncertainty and disagreement between the testing methodologies, depending on materials and even researchers.

In this study, the high-temperature slow-crack-growth behaviour of hot-pressed silicon carbide was determined using both constant-stress-rate and constant-stress testing at 1300 °C in air. The flexural test specimens were used under a four-point loading configuration. A total of 20 specimens was used at each test condition (i.e., 20 at each stress rate in constant-stress-rate testing, and 20 at each applied stress in constant-stress testing) to obtain statistically reliable strength and time-to-failure data. Several different estimation methods including the CARES/LIFE computer code recently developed at the Lewis Research Center, National Aeronautics and Space Administration, were utilized to determine the slow-crack-growth parameters from the results of constant-stress-rate and constant-stress testing.

2. Experimental procedure

The high-temperature slow-crack-growth behaviour of a hot-pressed silicon carbide material was determined in flexure via constant-stress-rate ("dynamic fatigue") and constant-stress ("static fatigue") testing. The material used in this study was hot-pressed silicon carbide (NC 203) fabricated by Norton Company (vintage 1981). The nominal dimensions of the flexural test

* To whom all correspondence should be addressed.
Present address: Lewis Research Center, National Aeronautics and Space Administration, Cleveland, OH 44135, USA.

specimens were 5.08 mm by 2.54 mm by 25 or 50 mm in width, height and length, respectively. The major room-temperature physical and mechanical properties of the material such as Young's modulus, density and fracture toughness are shown in Table I. The microstructure of the material is shown in Fig. 1. Equiaxed grains ranged in size from 1 to 10 μm with an average grain size of 4 μm. The primary second phase of the material was previously found to be alumina as a residual grain-boundary phase [9, 10].

Constant-stress-rate testing was carried out initially at 1200 °C in air. The testing was conducted using a SiC four-point flexure fixture with 20 mm inner and 40 mm outer spans in an electromechanical testing machine (Instron model 8562). Two loading rates of 2.0 N min^{-1} and 2000 N min^{-1}, corresponding to stress rates of 1.8 MPa min^{-1} and 1800 MPa min^{-1}, respectively, were used at 1200 °C. Five specimens were tested at each loading rate. However, no slow crack growth was observed at 1200 °C; so the test temperature was increased to 1300 °C where slow crack growth was evident. At 1300 °C, four loading rates of 3.65 N min^{-1}, 36.5 N min^{-1}, 365.0 N min^{-1} and 3650 N min^{-1}, corresponding to stress rates of 2 MPa min^{-1}, 20 MPa min^{-1}, 200 MPa min^{-1} and 2000 MPa min^{-1} respectively, were employed. A SiC four-point flexure fixture with 10 mm inner and 22 mm outer spans was used. Fast fracture strength was determined at 20 000 MPa min^{-1}. A total of 20 specimens was used at each stress rate. Constant-stress testing was conducted at 1300 °C in air. The testing machine and the test fixture were the same as those used for the constant-stress-rate testing at 1300 °C. Four different applied stresses ranging from 300 to 395 MPa were utilized. A total of 20 specimens was used at each applied stress. Each specimen was kept at test temperature for about 20 min prior to testing. Optical fractography and limited electron fractography were performed on the specimens to determine the source of fracture and degree of slow crack growth.

TABLE I Young's modulus, density and fracture toughness of NC 203 silicon carbide at room temperature

Young's modulus[a] (GPa)	Density[b] (g cm^{-3})	Fracture toughness[c] K_{Ic} (MPa m$^{1/2}$)
443 ± 2	3.31 ± 0.01	3.99 ± 0.20

[a] By the impulse excitation technique, ASTM C 1259 (with 31 flexural specimens).
[b] By the specimen mass/volume method (with 31 specimens).
[c] By the single-edge pre-cracked beam method (with five specimens).

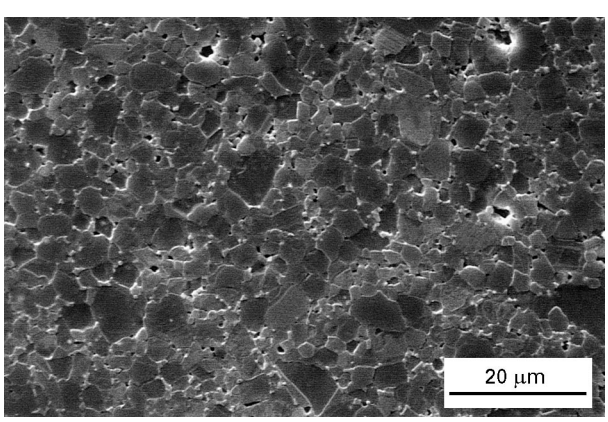

Figure 1 Microstructure of NC 203 silicon carbide.

3. Results and discussion

3.1. Constant-stress-rate testing

For most glass and advanced ceramics, the slow crack growth rate, v, can be expressed by the empirical power-law relation [11]

$$v = \frac{da}{dt} = A\left(\frac{K_I}{K_{Ic}}\right)^n \quad (1)$$

where a is the crack size, t is time, A and n are the slow-crack-growth parameters associated with material and environment, K_I is the mode I stress intensity factor, and K_{Ic} is the fracture toughness of the material under mode I loading. For constant-stress-rate testing which employs constant loading rates or constant cross-head speeds, the corresponding strength, σ_f, is expressed as [5]

$$\sigma_f = D\dot{\sigma}^{1/(n+1)} \quad (2)$$

where $\dot{\sigma}$ is the applied stress rate and D is the parameter which depends on n, inert strength (strength with no slow crack growth), fracture toughness and crack geometry factor. The slow-crack-growth parameters, n and D, can be obtained by a linear regression analysis from the slope and intercept, respectively, of the curve in which strength ($\log \sigma_f$) is plotted as a function of stress rate ($\log \dot{\sigma}$). In turn, the parameter A in Equation 1 can be obtained from D with the appropriate parameters [1].

A summary of the results of constant-stress-rate testing is presented in Table II. As seen in the table, the decrease in strength with decreasing stress rate, which represents slow-crack-growth susceptibility, was not significant at 1200 °C. This can be seen more clearly in a strength versus stress-rate curve (Fig. 2). At this temperature, the material exhibited almost no slow crack growth with a large slow-crack-growth parameter, $n = 108$. This is consistent with a previous result determined by Quinn [12] using constant-stress ("stress rupture") testing. It is believed that grain-boundary sliding, which is the mechanism responsible for slow crack growth at elevated temperatures, was not active at this temperature. Although alumina was found as a major secondary phase for this material [9], certain impurities (such as CaO) present in the material also were demonstrated to have a dramatic effect in slow-crack-growth behaviour, even with a slight change in test temperature [9, 10].

A decrease in strength with decreasing stress rate was now observed at 1300 °C. Extensive testing was conducted at this temperature using 20 specimens at each stress rate with a total of four stress rates. The results of constant-stress-rate testing are presented in Table II. The results are also depicted in the strength versus stress-rate curve ($\log \sigma_f$ versus $\log \dot{\sigma}$), as shown

TABLE II A summary of constant-stress-rate testing results of NC 203 silicon carbide in flexure at 1200 and 1300 °C in air

Temperature (°C)	Number of specimens	Stress rate, $\dot{\sigma}$ (MPa min^{-1})	Mean strength[a], σ_f (MPa)	Weibull parameters		
				Weibull modulus, m	Intercept (ln(MPa))	Weibull median strength (MPa)
1200	5	18	399.0 (35.5)	—	—	—
1200	5	1800	425.1 (35.6)	—	—	—
1300	20	2	351.3 (43.4)	9.65	57.08	355.90
1300	20	20	365.0 (64.9)	6.75	40.27	370.28
1300	20	200	390.5 (59.7)	7.69	46.34	395.91
1300	20	2000	445.4 (35.4)	15.02	92.11	449.90
1300	20	20 000	499.6 (40.9)	14.39	89.96	504.83

[a]The values in parentheses represent ± one standard deviation.

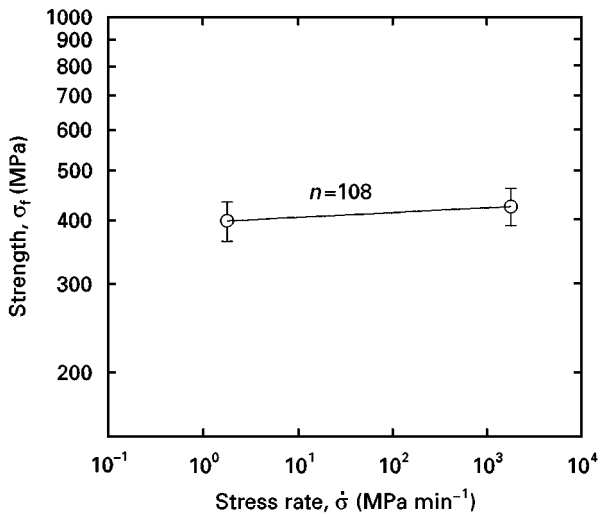

Figure 2 Results of constant-stress-rate ("dynamic fatigue") testing of NC 203 silicon carbide in flexure at 1200 °C in air. The solid line represents the best-fit line based on Equation 2 with the mean strength data. The error bar is ± one standard deviation.

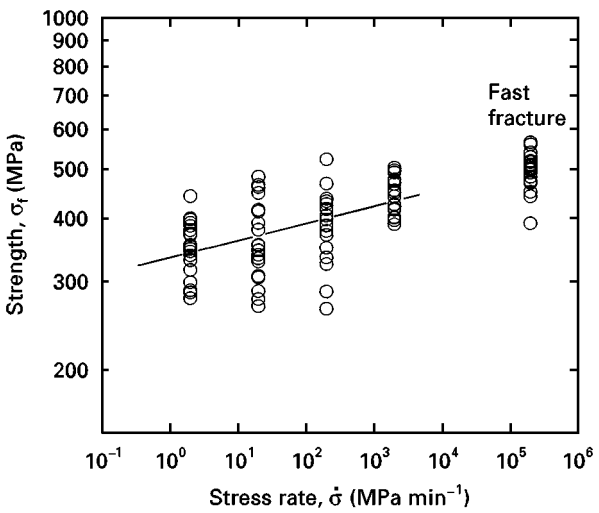

Figure 3 Results of constant-stress-rate ("dynamic fatigue") testing of NC 203 silicon carbide in flexure at 1300 °C in air. The solid line represents the best-fit line based on Equation 2 with the mean strength data.

in Fig. 3. The slow-crack-growth parameter, evaluated with Equation 2 and the mean strength values, was $n = 28.6 \pm 5.7$. Note that increasing the temperature from 1200 to 1300 °C makes a great difference in the slow-crack-growth behaviour of the material. As mentioned before, this is presumably due to the unique characteristics of grain-boundary phases and impurities in response to slow crack growth [9, 10], indicating that the transition of slow crack growth of the material lies between 1200 and 1300 °C.

The evaluation of the slow-crack-growth parameter, A, in Equation 1 requires a value of "inert" strength (i.e., the strength for which no crack extension occurs) [1]. The numerical solution of strength as a function of stress rate for natural flaws showed that the strength converges with increasing stress rate to a specific value defining the inert strength [13, 14]. Hence, high-temperature constant-stress-rate testing with a series of very high stress rates is required to eliminate or minimize slow crack growth so that, in principle, the strength convergence is reached, and the "inert" strength measured. It has been shown that a series of constant-stress-rate tests at stress rates equal to or greater than 2×10^6 MPa min^{-1} was required to reach convergence for ceramic materials [13]. Furthermore, in some cases, the value of convergence was found to be close to the room-temperature strengths of the materials. A series of very high stress rates, however, was not employed in this study because of the limited number of test specimens. Instead, only one stress rate of 20 000 MPa min^{-1} was used, and the corresponding strength was considered as a fast-fracture (or "inert") strength.

The two-parameter Weibull strength distributions, using $\ln\{\ln[1/(1-F)]\} = m\ln\sigma_f - \text{intercept}$ (with F and m being the failure probability and Weibull modulus, respectively), were obtained at each stress rate at 1300 °C and are presented in Fig. 4. The Weibull parameters based on the least-squares method are summarized in Table II. The Weibull moduli were estimated to be 9.7, 6.8, 7.7 and 15.0 at stress rates of 2 MPa min^{-1}, 20 MPa min^{-1}, 200 MPa min^{-1} and 2000 MPa min^{-1}, respectively. These Weibull moduli are within the range (7–15) commonly observed for most silicon nitride and carbide ceramics at elevated temperatures. It should be noted that the Weibull modulus was high ($m =$ 15) at 2000 MPa min^{-1} but low ($m = 7$–10) at

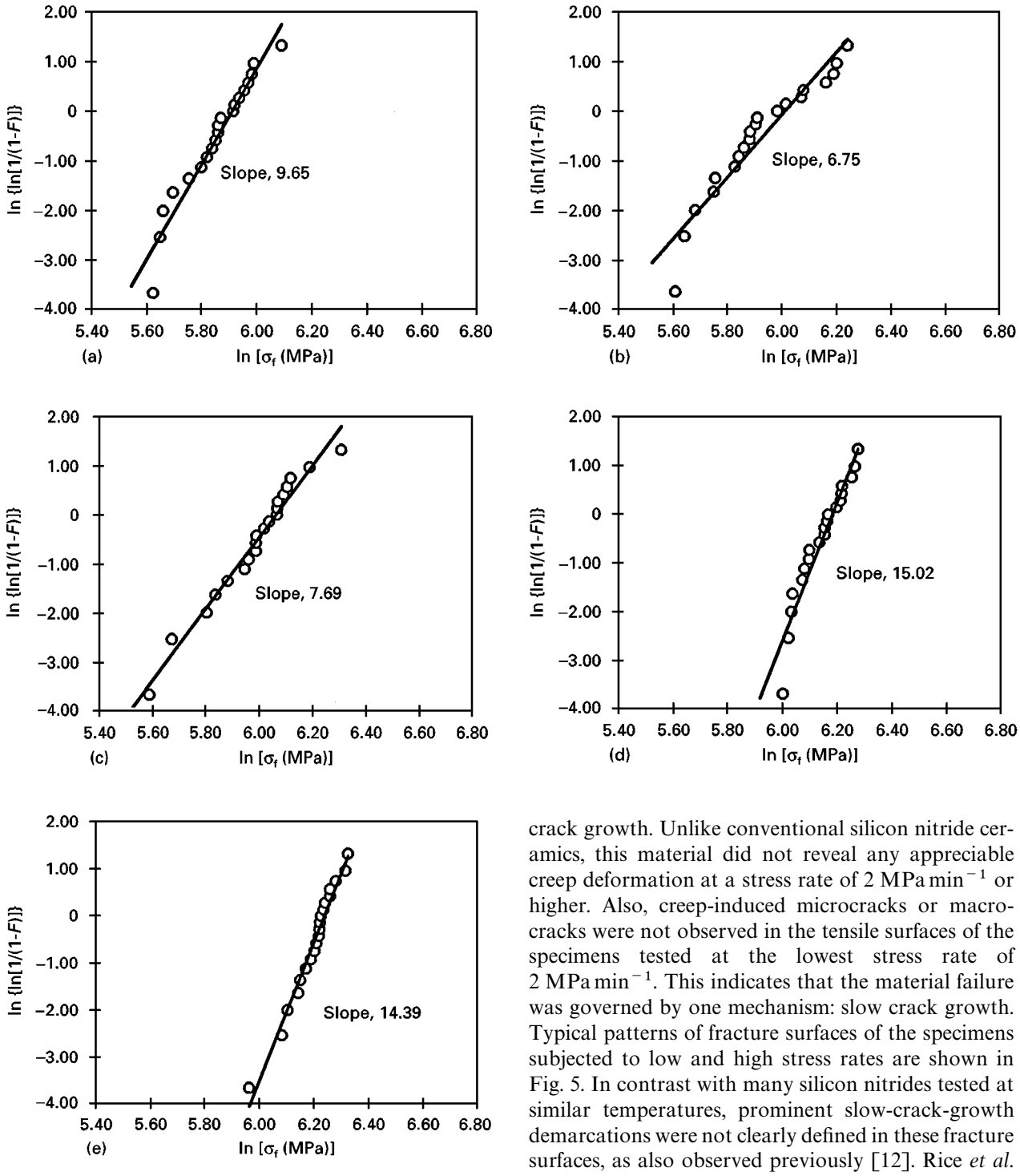

Figure 4 Weibull strength distributions for different stress rates obtained for NC 203 silicon carbide in flexure at 1300 °C in air: (a) 2 MPa min^{-1}; (b) 20 MPa min^{-1}; (c) 200 MPa min^{-1}; (d) 2000 MPa min^{-1}; (e) 20 000 MPa min^{-1} (fast-fracture strength).

2–200 MPa min^{-1}. If test specimens are reasonably randomized, then the Weibull moduli, m_f, in the slow-crack-growth regime should be consistent and higher than that of the Weibull moduli m_i, of the fast-fracture or "inert" strength data, regardless of stress rate, since [15]

$$m_f = \frac{m_i(n-1)}{n-2} \tag{3}$$

Fracture surfaces of the specimens tested at 1300 °C at lower stress rates generally revealed regions of slow crack growth. Unlike conventional silicon nitride ceramics, this material did not reveal any appreciable creep deformation at a stress rate of 2 MPa min^{-1} or higher. Also, creep-induced microcracks or macrocracks were not observed in the tensile surfaces of the specimens tested at the lowest stress rate of 2 MPa min^{-1}. This indicates that the material failure was governed by one mechanism: slow crack growth. Typical patterns of fracture surfaces of the specimens subjected to low and high stress rates are shown in Fig. 5. In contrast with many silicon nitrides tested at similar temperatures, prominent slow-crack-growth demarcations were not clearly defined in these fracture surfaces, as also observed previously [12]. Rice *et al.* [16] pointed out that the onset of dominant slow crack growth markings occurred only at temperatures of 1650 °C or higher. However, a careful examination of the fracture surfaces in terms of the mode of transgranular and intergranular failure showed different degrees of slow crack growth, which is consistent with the curve shown in Fig. 3.

3.2. Constant-stress testing ("static fatigue" or "stress rupture")

For constant-stress testing which employs a constant applied stress, σ, the corresponding time to failure, t_f, is expressed as [1]

$$t_f = G\sigma^{-n} \tag{4}$$

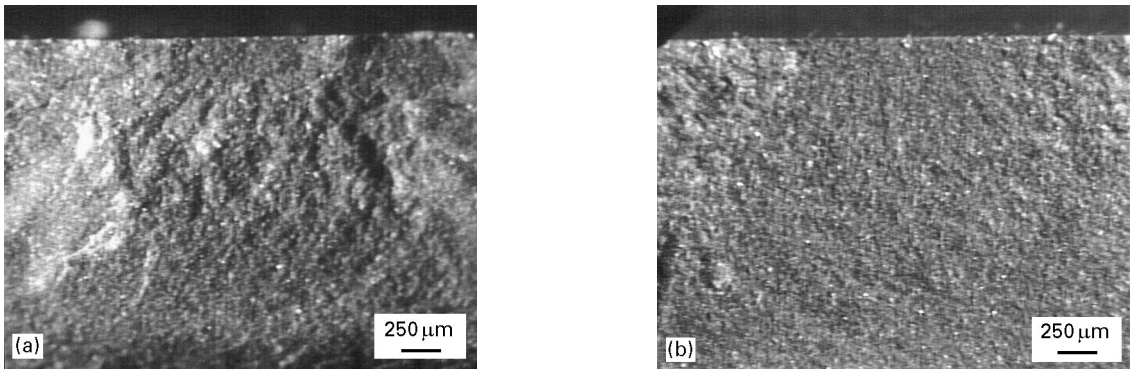

Figure 5 Typical fracture surfaces of NC 203 silicon carbide specimens subjected to constant-stress-rate ("dynamic fatigue") testing in flexure at 1300 °C in air: (a) 2000 MPa min^{-1}, $\sigma_f = 454.7$ MPa; (b) 2 MPa min^{-1}, $\sigma_f = 316.3$ MPa.

TABLE III A summary of constant-stress testing results of NC 203 silicon carbide in flexure at 1300 °C in air

Applied stress, σ (MPa)	Number of specimens	Mean time to failure[a], t_f (s)	Weibull parameters		
			Weibull modulus, m_{sf}	Intercept (ln(s))	Weibull median time to failure (s)
395	20	16.4 (21.8)	0.70	1.769	7.5
360	20	187.1 (420.3)	0.60	2.640	45.6
330	20	5020.9 (17632.3)	0.45	3.035	356.9
300	20	87228.6 (369414.5)	0.34	2.571	677.0

[a]The values in parentheses represent ± one standard deviation.

where G is a parameter associated with n, the inert strength, the fracture toughness and the crack geometry factor. The slow-crack-growth parameters, n and G, can be obtained by a linear regression analysis from the slope and intercept, respectively, of the curve in which the time to failure ($\log t_f$) is plotted as a function of applied stress ($\log \sigma$). From G, the parameter A can be estimated with the appropriate parameters [1].

A summary of the constant-stress test results is presented in Table III. The Weibull parameters (the Weibull modulus, m_{sf}, the intercept and the Weibull median time to failure), based on the least-squares method in a two-parameter scheme of $\ln\{\ln [1/(1-F)]\} = m_{sf} \ln t_f -$ intercept, are also included in the table. The decrease in time to failure with increasing applied stress, which represents slow-crack-growth susceptibility, is evident, as seen in the table. The resulting plot of $\log t_f$ versus $\log \sigma$, based on Equation 4, is shown in Fig. 6. The slow-crack-growth parameter was found to be $n = 31.8 \pm 1.5$ based on Equation 4 in conjunction with the mean time-to-failure data.

The Weibull time-to-failure distributions obtained at each applied stress are presented in Fig. 7. The Weibull moduli m_{sf} was estimated to be 0.70, 0.60, 0.45 and 0.34 at applied stresses of 395 MPa, 360 MPa, 330 MPa and 300 MPa, respectively, resulting in an average value of $m_{sf} = 0.52 \pm 0.16$. The Weibull modulus, m_{sf}, is related to the Weibull modulus, m_i, of inert strength as follows [1]:

$$m_{sf} = \frac{m_i}{n-2} \tag{5}$$

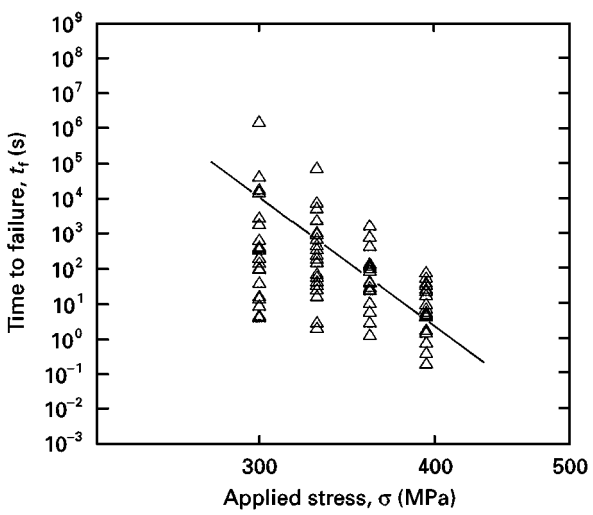

Figure 6 Results of constant stress ("static fatigue" or "stress rupture") testing of NC 203 silicon carbide in flexure at 1300 °C in air. The solid line represents a prediction from the arithmetic mean data obtained from the constant-stress-rate testing.

Using $n \approx 30$ and $m_i \approx 14$ from Table II, a value of $m_{sf} = 0.5$ was obtained, which is in reasonable agreement with the average value of 0.52 determined from the results in Fig. 7. However, it should be noted that the individual Weibull moduli determined from the constant-stress testing (see Table III) were not consistent but changed appreciably from 0.70 to 0.34 with decreasing applied stress. Also note that the Weibull time-to-failure distribution seems to be bimodal rather than unimodal, as can be seen in Fig. 7.

Fracture surfaces of the specimens tested at lower applied stresses generally revealed regions of slow

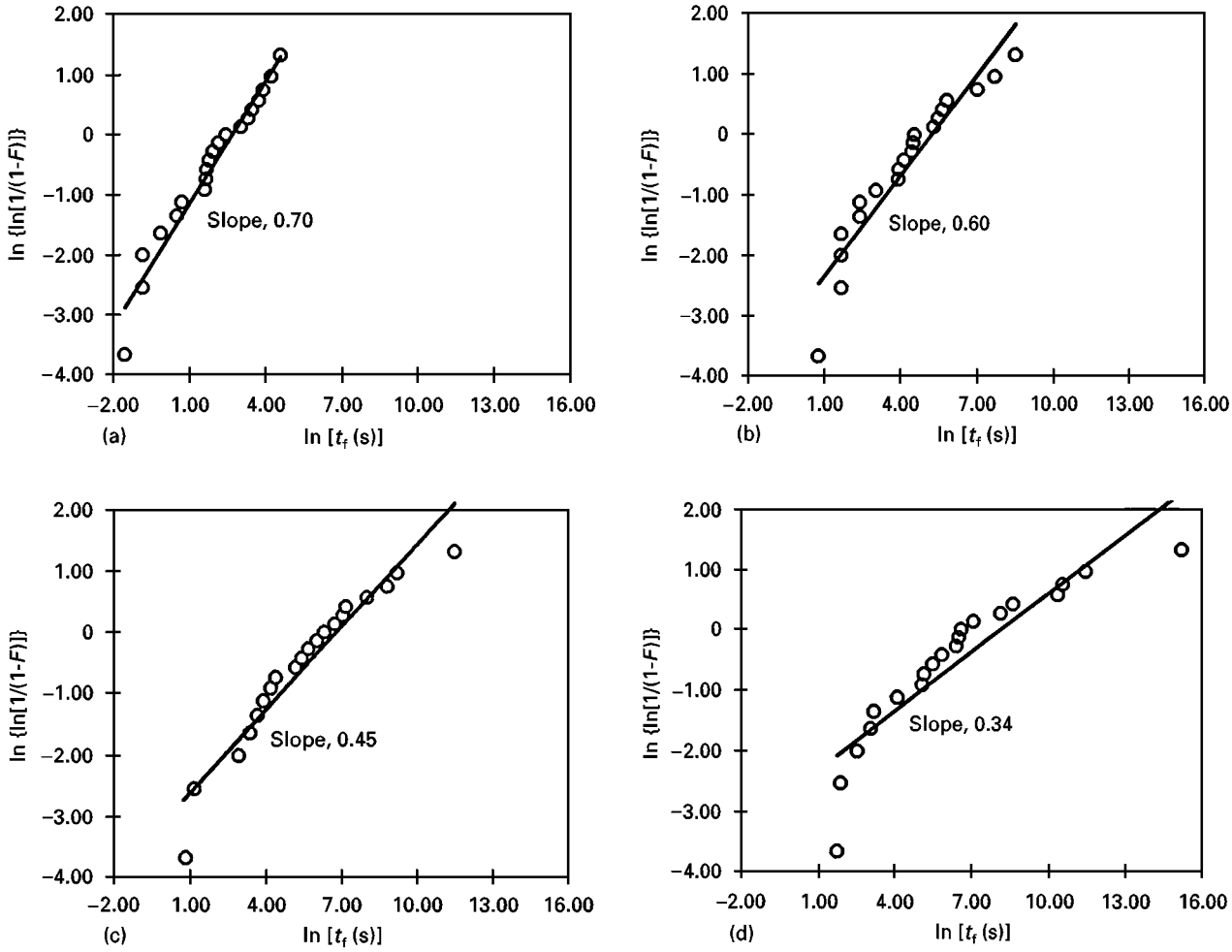

Figure 7 Weibull time-to-failure distributions for different applied stresses obtained for NC 203 silicon carbide at 1300 °C in air: (a) 395 MPa; (b) 360 MPa; (c) 330 MPa; (d) 300 MPa.

crack growth. The material did not exhibit any appreciable creep deformation even at the lowest applied stress (300 MPa) with a very long time to failure. For example, the creep deformation was found to be less than 0.1% for the specimen subjected to the lowest applied stress, $\sigma = 300$ MPa, with a long test time, $t_f = 460$ h. Also, creep-induced microcracks or macrocracks were not observed in the tensile surfaces of the specimens tested at 300 MPa, indicating that slow crack growth was a governing mechanism associated with failure in the constant-stress testing. Typical fracture surfaces and their corresponding tensile surfaces for the specimens subjected to low and high applied stresses are shown in Fig. 8.

3.3. Comparison of lifetime prediction parameters between constant-stress-rate testing and constant-stress testing

The lifetime of a ceramic component for a given applied load is a strong function of the slow-crack-growth parameter, n, as can be seen from the functional form of Equation 4. Therefore, the accurate determination of n is of great importance so that the lifetime prediction of the component is reasonably ensured. Currently, several statistical methods are available to estimate the slow-crack-growth parameters. These include the arithmetic mean, the Weibull median, the median deviation, the individual (all) data, the homologous stress and the bivariant and trivariant methods [17–19]. Basically, most of the techniques utilize the least-squares best-fit analysis based on the appropriate formulae: Equation 2 for constant-stress-rate testing and Equation 4 for constant-stress testing. The maximum likelihood estimation method using either median or individual data has recently been used by Gross *et al.* [19]. Each method possesses its own advantages and disadvantages over other methods. However, the estimated parameters are to be converged to the similar values, independent of the estimation method, if a sufficient number of test specimens (20–40 or more, depending on the Weibull modulus) are used. Also, it is important to note that the estimation method should be simple and convenient to use with few complications. This is particularly significant when a test method is to be standardized to determine the slow-crack-growth parameters of a material.

Three simple and convenient estimation methods were used in this study to determine the slow-crack-growth parameter, n. These were the individual data

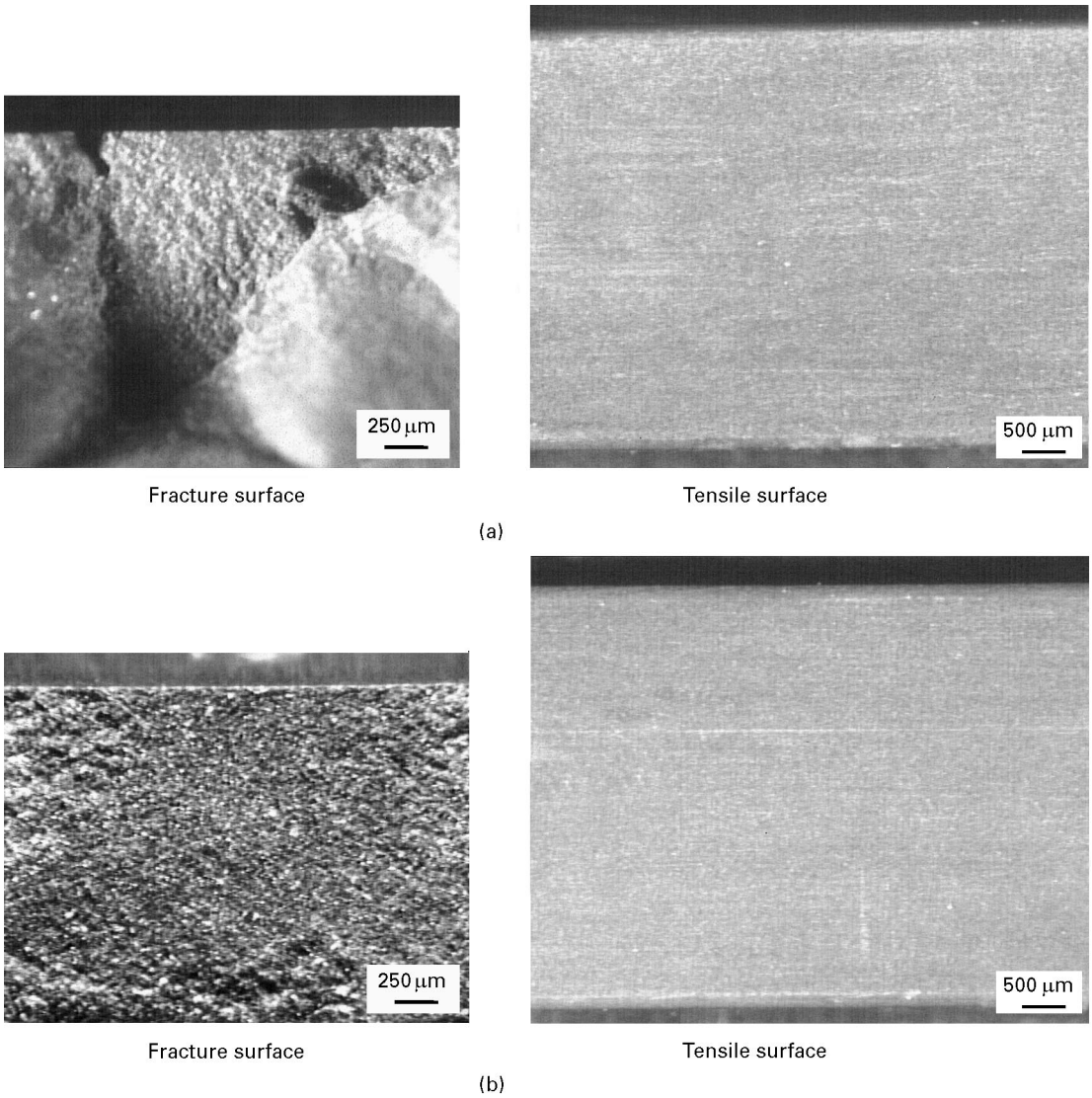

Figure 8 Typical fracture surfaces and tensile surfaces of NC 203 silicon carbide specimens subjected to constant stress ("static fatigue") testing in flexure at 1300 °C in air: (a) $\sigma = 395$ MPa, $t_f = 1.5$ s; (b) $\sigma = 300$ MPa, $t_f = 460$ h.

method, the Weibull median data method and the arithmetic mean method. In the individual data method, each individual strength value obtained at each corresponding stress rate is used in constant-stress-rate testing, while each individual time to failure obtained at each applied stress is utilized in constant-stress testing. In the Weibull median data method, the Weibull median strength at each stress rate and the Weibull median time to failure at each applied stress are used in constant-stress-rate and constant-stress testing, respectively. The Weibull median method can be meaningful only when the number of test specimens is at least 20 for typical advanced ceramics. The arithmetic mean method utilizes the arithmetic mean strength and the arithmetic mean time to failure in constant-stress-rate and constant-stress testing, respectively. The median deviation method which was used for comparison in this study is a measure of the spread of the data about the median value. This approach is used when the inert parameters are unknown and only constant-stress slow-crack-growth data are available [19]. The CARES/LIFE code has a greater flexibility and can be used in several different estimation methods including the median deviation method.

A summary of the slow-crack-growth parameter, n, obtained from the four different methods is shown in Table IV. In constant-stress-rate testing, the estimation methods based on the individual strength, the Weibull median and the arithmetic mean strength data yield an almost consistent value of $n = 28$–29, whereas the CARES/LIFE median deviation gives $n = 36$. However, the variation between n from these methods is not significant, ranging from $n = 28$ to $n = 36$. In constant-stress testing, the CARES/LIFE median deviation ($n = 27.4$) and the arithmetic mean ($n = 31.8$) methods are in good agreement but they are in poor agreement with the individual data ($n = 15.9$) or the Weibull median ($n = 17.0$) method. This contrasts with the results obtained by the constant-stress-rate testing, where a narrow range $n = 28$–36 was observed, regardless of evaluation method. The CARES/LIFE median deviation or the arithmetic mean method is preferred, as they are consistent with the constant-stress-rate testing results. However, the best agreement was found in the

TABLE IV Comparison of the slow-crack-growth parameter, n, from four different estimation methods for NC 203 silicon carbide in constant-stress-rate and constant-stress testing in flexure at 1300 °C in air

Method	Slow-crack-growth parameter, n	
	Constant-stress-rate testing	Constant-stress testing
Individual data (CARES/LIFE least squares)	28.0 ± 5.1	15.9 ± 2.7
Weibull median	28.8 ± 6.0	17.0 ± 2.7
Arithmetic mean	28.6 ± 5.7	31.8 ± 1.5
CARES/LIFE median deviation	36.1	27.4

arithmetic mean method. The prediction of lifetime based on the constant-stress-rate test data (arithmetic mean data) is shown as a solid line in Fig. 6.

Good agreement between the n values obtained by the estimation methods in constant-stress-rate testing also indicates that statistical reproducibility [15] is better in the data obtained from constant-stress-rate testing than in those from constant-stress testing. The very large standard deviations in the mean time to failure data, as shown in Table III, are indicative of such poor statistical reproducibility. Also note the large scatter in t_f (time to failure), particularly at the lowest applied stress of 300 MPa, ranging from one to seven orders of magnitude (see Fig. 6). The scatter increased with decreasing applied stress. Although the slow-crack-growth phenomenon was a governing failure mechanism associated with the constant-stress testing, a change in flaw populations and/or configurations might occur presumably owing to oxidation, flaw healing and/or flaw blunting at the test temperature with decreasing applied stress. It is believed that this change in flaw populations and/or configurations might result in such a wide scatter in the time-to-failure data. Also note the possible bimodal Weibull time-to-failure distributions in Fig. 7, probably indicative of the occurrence of such a flaw and/or geometry change.

4. Conclusions

Slow crack growth was found to be a governing mechanism associated with failure of NC 203 silicon carbide tested in flexure at 1300 °C in air, either in constant-stress-rate testing or in constant-stress testing. The four estimation methods such as the individual data, the Weibull median, the arithmetic mean and the median deviation methods were in good agreement for constant-stress-rate testing with a small variation in slow-crack-growth parameter n, ranging from $n = 28$ to $n = 36$. By contrast, the variation in n between the four estimation methods in constant-stress testing was significant with $n = 16$–32. The best agreement between the constant stress-rate and the constant-stress testing was found in the arithmetic mean method: $n = 29 \pm 6$ for constant-stress-rate testing and $n = 32 \pm 2$ for constant-stress testing.

Acknowledgements

This research was sponsored in part by the Ceramic Technology Project, US Department of Energy Office of Transportation Technologies, under Contract DE-AC05-84OR21400 with Martin Marietta Energy Systems, Inc. The authors are grateful to R. Pawlik at Lewis Research Center, National Aeronautics and Space Administration, for experimental and scanning electron microscopy work.

References

1. J. E. RITTER, in "Fracture mechanics of ceramics", Vol. 4, edited by R. C. Bradt, D. P. H. Hasselman and F. F. Lange (Plenum, New York, 1978) p. 667.
2. G. G. TRANTINA, *J. Amer. Ceram. Soc.* **62** (1979) 377.
3. R. K. GOVILA, *ibid.* **65** (1982) 15.
4. G. D. QUINN and J. B. QUINN, in "Fracture mechanics of ceramics", Vol. 6, edited by R. C. Bradt, A. G. Evans, D. P. Hasselman and F. F. Lange (Plenum, New York, 1983) p. 603.
5. A. G. EVANS, *Int. J. Fract.* **10** (1974) 251.
6. S. R. CHOI, J. A. SALEM and J. L. PALKO, in "Life prediction methodologies and data for ceramic materials", ASTM Special Technical Publication 1201, edited by C. R. Brinkman and S. F. Duffy (American Society for Testing and Materials, Philadelphia, PA, 1994) p. 98.
7. L. CHUCK, D. E. McCULLUM, N. L. HECHT and S. M. GOODRICH, *Ceram. Engng Sci. Proc.* **12** (1991) 1509.
8. A. G. EVANS and S. M. WIEDERHORN, *J. Mater. Sci.* **9** (1974) 270.
9. D. G. MILLER *et al.*, US Army Materials and Mechanics Research Center, Watertown, MA, Technical Report CTR 76-32 (1976).
10. A. G. EVANS and F. F. LANGE, *J. Mater. Sci.* **10** (1975) 1659.
11. S. M. WIEDERHORN, in "Fracture mechanics of ceramics", Vol. 2, edited by R. C. Bradt, D. P. H. Hasselman and F. F. Lange (Plenum, New York, 1974) p. 613.
12. G. D. QUINN, US Army Materials and Mechanics Research Center, Watertown, MA, Technical Report TR 80-15 (1980).
13. S. R. CHOI and J. A SALEM, *Mater. Sci. Engng* **A** (1997) in press.
14. *Idem.*, *Ceram. Engng Sci. Proc.* **17** (1996) 454.
15. J. E. RITTER, N. BANDYOPADHYAY and K. JAKUS, *Ceram. Bull.* **60** (1981) 798.
16. R. RICE *et al.*, in "Ceramics for high performance applications II", edited by J. J. Burke, E. M. Lenoe and R. N. Katz (Brook Hill Publishing, Chestnut Hill, MA, 1978) p. 669.
17. K. JAKUS, D. C. COYNE and J. E. RITTER, *J. Mater. Sci.* **13** (1978) 2071.
18. N. N. NEMETH, L. M. POWERS, L. A. JANOSIK and J. P. GYEKENYESI, in "Life prediction methodologies and data for ceramic materials", ASTM Special Technical Publication 1201, edited by C. R. Brinkman and S. F. Duffy (American Society for Testing and Materials, Philadelphia, PA, 1994) p. 390.
19. B. GROSS, L. M. POWERS, O. M. JADAAN and L. A. JANOSIK, Lewis Research Center, National Aeronautics and Space Administration, Cleveland, OH, Technical Memorandum 4699 (1996).

Received 31 October 1996
and accepted 14 October 1997